Numerical Study of a Solar Chimney Power Plant

Dr. Jalal M. Jalil
Electromechanical Engineering Department, University of Technology/Baghdad
Email: jalalmjalil@yahoo.com
Dr. Rafah A. Najim
Electromechanical Engineering Department, University of Technology/Baghdad

Received on: 19/2/2012 & Accepted on: 24/6/2012

ABSTRACT

Axi-symmetric, steady, incompressible, turbulent flow field developed by natural convection inside power plant solar chimney is investigated numerically using finite volume method. Navier-Stockes with energy equation is solved to achieve velocity components and temperature distribution inside solar chimney. To complete the thermal analysis, conduction through upper glass wall, chimney concrete wall and floor ground were investigated to calculate temperature distribution through theses walls. A standard **k - e** turbulence model associated with lawss of the wall along solid boundaries was used. Special arrangement for mesh was used to deal with complicated shape of the domain. The main studied parameters are solar collector diameter, kinds of ground, periphery heights and solar intensity radiation. This study was compared with previous available experimental study and there is acceptable agreement. The performance of the solar chimney was examined through maximum air velocity in the tower inlet and maximum temperature in the ground floor. The final optimization parameters are defined within studied ranges.

Keywords: Solar chimney, Finite volume, CFD, Induced flow, Natural convection

دراسة عددية لمدخنة شمسية لتوليد الطاقة

الخلاصة

درس البحث الحالي مدخنة شمسية لتوليد الطاقة الكهربائية وذلك باستخدام حقل جريان متماثل، لا انظغاطي واضطرابي لتيارات الحمل الطبيعي وحلها عدديا باستخدام طريقة العناصر المحددة لحل معادلة Navier-Stokes equation ومعادلات الطاقة وذلك لحساب مكونات السرعة وتوزيع درجة الحرارة. لانجاز التحليل الحراري تم حساب التوصيل خلال الجدار العلوي الزجاجي ، جدار المدخنة الاسمنتي والارضية الممتصة للمجمع الشمسي ولقد تم الاستعانة بالموديل الاضطرابي (k–ε) الذي ترافق حسابه مع قوانين الجدار على طول الحدود الصلبة، مع الاخذ بالاعتبار تدابير خاصة للتعامل مع الشكل المعقد للحقل. ولاختبار صلاحية الدراسة فقد تم مقارنتها مع دراسة عملية سابقة ولنفس الظروف المحيطة، وكان هناك توافق مقبول ما بينهما. لقد اختبر اداء المدخنة الشمسية خلال اعلى سرعة للهواءفي مدخل المدخنة و اعلى درجة حرارة في الارضية ولقد جرى تحديد العوامل المثالية ضمن المدى المدروس.

https://doi.org/10.30684/etj.30.15.4
2412-0758/University of Technology-Iraq, Baghdad, Iraq

Symbol	*Description*	*Unit*
A_e, A_w, A_n , A_s	Cross section area of cell faces	m^2
C_e, C_w, C_s, C_n	Coefficients of Conduction and Convection	
G	Kinetic energy generation by shear	J
H_g, H_w, H_{w1},H_s	Thickness of glass, absorbing ground, chimney wall and soil underneath respectively.	m
h_o, h_{in}	Heat transfer coefficient outside and inside collector respectively.	
i,j	Unit vectors in position (x, r) direction respectively.	
k_g, k_w, k_{w1},k_s	Thermal conductivity of glass, absorbing ground, chimney wall and soil underneath respectively.	W/m^oC
q_E, q_W, q_S, q_N	Total heat flow	W
R	Solar radiation reflected	W/m^2
Δx , Δr	Physical cell dimensions(i.e. distance between cell-faces)in cylindrical coordinate	m
e	Rate of dissipation of kinetic energy	m^2/s^2
l	Ratio of solar radiation reflect =0.020	
r	Fluid density	kg/m^3
f	General dependent variable	
m	Dynamic viscosity	$N.s/m^2$
m_t	Turbulent viscosity	$N.s/m^2$
m_{eff}	Effective kinematics viscosity	$N.s/m^2$
G	Diffusion coefficient, $G = m / s$	$N.s/m^2$
Γ_{eff}	Effective diffusion coefficient	$N.s/m^2$
x, r	Cylindrical coordinate	m
S_u, S_v, S_T, S_k, S_p	Coefficients of lineairzed source expression	
P	Pressure	N/m^2
u, v	Velocity components (x& r) direction	m/s

INTRODUCTION

The principle of solar chimney (shown in Figure 1) is to convert the solar radiation into another type (kinetic energy) in which the air is heated and expanded under large glass roof. This flows to a chimney in the middle of the roof and is drawn upwards this updraft. Drives turbines are installed at the base of the chimney, and these produce electricity, William, 2002.

Many studies about solar energy applications have been carried out, some of which became true, yet the others are still in the process of development. Ronald, 2002 studied theoretical wind power from a sun with (12.566×10^6) m^2 area of solar collector. Ong**,** 2002 proposed a simple mathematical model of a solar chimney, steady state heat transfer equations are set up to determine the boundary temperatures. Bilgen, 2005 have developed a mathematical model and a code on MATLAB platform on monthly average meteorological data and thermodynamic cycle. Pretorius, 2005 compared computer simulation to study evaluation of the influence of a recently developed convective heat transfer equation. Adam, 2005 produced a mathematical simulation and experimental investigation of airflow in solar chimney which was a simple channel glazed on one with a collector wall on the other. Zhou, 2006 investigated the performance of a pilot experimental solar chimney setup in China. Zhou, 2006 studied experimental solar chimney power setup consisting of a 5 m-radius air collector and an 8m-height chimney.

The aim of this work is to develop a numerical study to calculate the flow characteristics (distribution of temperature and air velocity) for a solar chimney to generate electricity. The work deals with many variables such as: solar intensity radiation (300-700 W/m^2), periphery heights (0.08-0.16 m), absorbent ground (asphalt aggregates, marbles and sandstones) and collector diameters (6, 7, 8 and 9 m). Other fixed parameters are the chimney height and diameter (6, 0.3 m) respectively.

MATHEMATICAL FORMULATIONS

Air Flow Domain inside the Solar Chimney

The working fluid (air) is allowed to flow freely between the cover and the absorber. The collector has a circular shape. Most practical problems which deal with subjects of flow field and heat transfer are governed by principles of conservation of mass, momentum and energy. These principles can be expressed in terms of partial differential equations, which will be presented in the form of cylindrical coordinates, 2-D (axi-symmetric), steady flow:

i- Continuity equation (mass conservation)

$$\frac{\partial}{\partial x}(rru) + \frac{\partial}{\partial r}(rrv) = 0 \qquad \text{……..(1)}$$

ii - Momentum equations:

u-Momentum (x-direction)

$$\frac{1}{r}\left[\frac{\partial}{\partial x}(rruu) + \frac{\partial}{\partial r}(rrvu)\right] = -\frac{\partial p}{\partial x} + \frac{1}{r}\left[\frac{\partial}{\partial x}\left(rm_{eff}\frac{\partial u}{\partial x}\right) + \frac{\partial}{\partial r}\left(rm_{eff}\frac{\partial u}{\partial r}\right)\right] + S_u \qquad \text{……. (2)}$$

v-Momentum (r-direction)

$$\frac{1}{r}\left[\frac{\partial}{\partial x}(rruv)+\frac{\partial}{\partial r}(rrvv)\right]=-\frac{\partial p}{\partial r}+\frac{1}{r}\left[\frac{\partial}{\partial x}\left(rm_{eff}\frac{\partial v}{\partial x}\right)+\frac{\partial}{\partial r}\left(rm_{eff}\frac{\partial v}{\partial r}\right)\right]-m_{eff}\frac{v}{r^2}+S_V \quad \text{…. (3)}$$

iii - Energy Equation

$$\frac{1}{r}\left[\frac{\partial}{\partial x}(rruT)+\frac{\partial}{\partial r}(rrvT)\right]=\frac{1}{r}\left[\frac{\partial}{\partial x}\left(r\Gamma_{eff}\frac{\partial T}{\partial x}\right)+\frac{\partial}{\partial r}\left(r\Gamma_{eff}\frac{\partial T}{\partial r}\right)\right]+S_T \quad \text{… (4)}$$

Where:

$$S_u=\frac{\partial}{\partial x}\left(m_{eff}\frac{\partial u}{\partial x}\right)+\frac{1}{r}\frac{\partial}{\partial r}\left(rm_{eff}\frac{\partial v}{\partial x}\right) \quad \text{….. (5)}$$

$$S_v=\frac{\partial}{\partial x}\left(m_{eff}\frac{\partial u}{\partial r}\right)+\frac{1}{r}\frac{\partial}{\partial r}\left(rm_{eff}\frac{\partial v}{\partial r}\right)-m_{eff}\frac{v}{r^2} \quad \text{..... (6)}$$

$$m_{eff}=m+m_t \quad \text{..... (7)}$$

$$\Gamma_{eff}=\frac{m}{d}+\frac{m_t}{d_t} \quad \text{… (8)}$$

In equations 1 to 4, a mathematical expression for effective kinematics viscosity (ν_{eff}) and effective diffusion coefficient (Γ_{eff}) will be required through the use of turbulence model.

THE STANDARD k - e MODEL

The turbulence according to (Launder, 1972) is assumed to be characterized by its kinetic energy and dissipation rate (ε). This model relates the turbulent viscosity to the local values of ρ, k and ε by the expression.

$$m_t=r\,C_m\,k^2/e \quad \text{….. (9)}$$

Where $\mathbf{C}_m$ is an empirical "constant" value for high Reynolds number. The turbulence parameters k and e are derived from their respective transport equations:

i - Turbulence kinetic energy (k)*:*

$$\frac{1}{r}\left[\frac{\partial}{\partial x}(rruk)+\frac{\partial}{\partial r}(rrvk)\right]=\frac{1}{r}\left[\frac{\partial}{\partial x}\left(r\Gamma_k\frac{\partial k}{\partial x}\right)+\frac{\partial}{\partial r}\left(r\Gamma_k\frac{\partial k}{\partial r}\right)\right]+S_k \quad \text{.. (10)}$$

$$\Gamma_k = m_{eff} / d_k \quad \text{..... (11)}$$

$$S_k = G - C_D re \quad \text{..... (12)}$$

ii - Dissipation rate (e):

$$\frac{1}{r}\left[\frac{\partial}{\partial x}(rru\varepsilon)+\frac{\partial}{\partial r}(rrv\varepsilon)\right]=\frac{1}{r}\left[\frac{\partial}{\partial x}\left(\Gamma_e r\frac{\partial e}{\partial x}\right)+\frac{\partial}{\partial r}\left(\Gamma_e r\frac{\partial e}{\partial r}\right)\right]+C_1\frac{e}{k}G-C_2 r\frac{e^2}{k} \quad \text{..... (13)}$$

$$\Gamma_e = m_{eff} / d_e \quad \text{..... (14)}$$

Where:

$$G = m_t\left(2\left[\left(\frac{\partial u}{\partial x}\right)^2+\left(\frac{\partial v}{\partial r}\right)^2+\left(\frac{v}{r}\right)^2\right]+\left(\frac{\partial u}{\partial r}+\frac{\partial v}{\partial x}\right)^2\right)+S_G \quad \text{..... (15)}$$

$$S_G = \frac{-2}{3}m_t\left[\frac{1}{r}\frac{\partial}{\partial r}(rv)+\frac{\partial u}{\partial x}\right]^2 \quad \text{..... (16)}$$

The values of the empirical constant used here are given in Table 1. The conservation equation of mass, momentum and energy are solved by the SIMPLE algorithm with hybrid difference scheme. Non-uniform grids were employed, with 61 × 61 mesh.

Heat Conduction Through Walls

Analysis of Steady Heat Conduction of the Glass Solar Collector

An incline glass wall with thickness (6 mm) is to be analyzed by conduction equations. Sample of the nodes are shown in Figure (2). The inclined line of glass was represented by steps as shown in Figure (2) to simplify the problem. This approximation will allow use of Cartesian coordinates. The conduction equations are:

$$\sum_{Allside} q = q_E + q_W + q_S + q_N = 0 \quad \text{..... (17)}$$

$$q_E = k_g.A_e.\frac{(t_{(1)}-t_{(8)})}{H_g} \quad \text{.....(18a)}$$

$$q_W = h_o.A_w.(t_{(1)}-t_o) \quad \text{.....(18b)}$$

$$q_S = k_g.A_s\frac{t_{(1)}-t_{(2)}}{H_g} \quad \text{.....(18c)}$$

$$q_N = h_o . A_n . (t_{(1)} - t_o) \quad \text{.....(18d)}$$

$$A_e = 2 \times p \times (r_{(m)} + H_g) \times \frac{H_g}{2} \quad \text{..... (19)}$$

$$A_w = 2 \times p \times (r_{(m)} + H_g) \times \frac{H_g}{2} \quad \text{..... (20)}$$

$$A_n = 2 \times p \times (r_{(m)} + H_g) \times \frac{H_g}{2} \quad \text{.... (21)}$$

$$A_s = 2 \times p \times (r_{(m)} + \frac{H_g}{2}) \times \frac{H_g}{2} \quad \text{..... (22)}$$

The resulting Equation is:

$$t_{(1)} = t_{(1)} . (1-r) + r . [C_e . t_{(8)} + C_w . t_o + C_S . t_{(2)} + C_n . t_o + Q . (\frac{A_n}{2} + A_w)] \ / C_J \ . \quad \text{.... (23)}$$

Where:

$R = \lambda \ q_T$ .....(24)

$Q = R . q_T .$ ..... (25)

Where:

$$S = \frac{(\Delta r - H_g)}{2} \quad \text{.....(26)}$$

$$SS = \frac{(\Delta x - H_g)}{2} \quad \text{.....(27)}$$

The analysis of both chimney and absorption black ground walls is similar to the glass analysis mentioned-above.

RESULTS AND DISCUSSION

In order to validate the results of the present work, a comparison with an experimental work was carried out in Figures (3) and (4). In these figures, the variation of exit air velocity and temperatures with heat flux at 12 am, 2 pm and 4 pm for five days, using asphalt aggregates as an absorption black ground and 0.1 m periphery of collector. Acceptable agreement was achieved with Shyia, 2002.

The conversion from solar radiation into thermal energy is at the ground surface. The temperature in the center of the absorbing ground, mass flow rate and exit air velocity increases linearly with the increasing of solar radiation intensity for three kinds (sandstone, marble and asphalt aggregates), from the Figures (5) and (6), the asphalt aggregate is the better ground for absorption because of its physical properties.
The results show that the collector periphery height from the ground has a large effect on the performance from other factors which are flow field, isothermal distribution, mass flow rate, air temperature and exit air velocity as follows:

From Figures (7) and (8), (D =7, 9 m) and (L=0.16 m) periphery height, the flow field increases with increasing of the diameter and decreasing of solar chimney air temperature due to increasing of inlet air volume that draft the heat from the system and the air turbulence happens because of rotation. The air tends to rotate around any low pressure area counterclockwise in Northern hemisphere (Ronald, 2002). From Figures (9) and 10 at (D =7, 9 m) and (L=0.16 m) periphery height, air temperature will increase with increasing of diameter, but decreases periphery height (L=0.1m) because of much air mass that enters the chimney. The maximum exit air velocity was found at the smaller diameter because of temperature differences which cause air turbulence that cools some regions in the system, with heat flux (300-700 W/m^2) and (L= 0.10 m) , as in Figure (11). Maximum temperature in the center of the absorbing ground occurs at the larger diameter due to collector area exposed to the incident radiation, with heat flux (300-700W/m^2) and (L= 0.10 m), as in Figure (12).

CONCLUSIONS

1- The numerical results have good agreement with the experimental results of Shyia, 2002.
2- The better ground of the collector is Asphalt aggregates.
3- Maximum air temperature and maximum outlet air velocity both at collector roof height 0.1m.
4- Increasing in collector diameter leads to increase of air temperature.
5- The Increase in periphery height leads to increasing in incoming air volume and decreasing of absorbing ground temperature and then reduces the air velocity.

REFERENCES

[1].Adam, Z., Yamanaka, T. & Kotani, H. 2005. Mathematical model and Experimental study of airflow in solar chimneys. Osaka University, Japan.
[2].Bilgen, E. & Rheault, J. 2005. Solar chimney power plants for high latitudes. Montreal, Canada.
[3].Launder,B.,E., & Spalding,D.,B., 1972. Mathematical Models of turbulence, Academic press, London.
[4].Ong, K.S. 2002. A mathematical model of solar chimney. Monash University Malaysia, Malaysia.
[5].Pretorius, J.P.,Kröger,D.,G., 2005. Critical evaluation of solar chimney power plant performance. south Africa.
[6].Ronald, L., Jr., 2002. The wind from the sun power plant. www. Wind from the sun .com USA.
[7].Shyia, A., K., 2002. Parametric study of solar chimney performance. M.Sc. Thesis, University of AL-Mustansiriya.
[8].William, A. 2002, Solar Electricity night and day.
[9].Zhou, X., Yang, J., Xiao, B.& Hou, G., 2006. Simulation of a pilot solar chimney thermal power generating equipment. Huazhong University of Science and Technology, China.
[10].Zhou, X., Yang, J., Xiao, B. & Hou, G., 2006. Experimental study of the temperature field in a solar chimney power setup. Huazhong University of Science and Technology, China.

Table(1) Values of constants in the $(k-\varepsilon)$ model [12]

C_m	C_D	C_1	C_2	δ_k	δ_ε
0.09	1.00	1.44	1.92	1.0	1.3

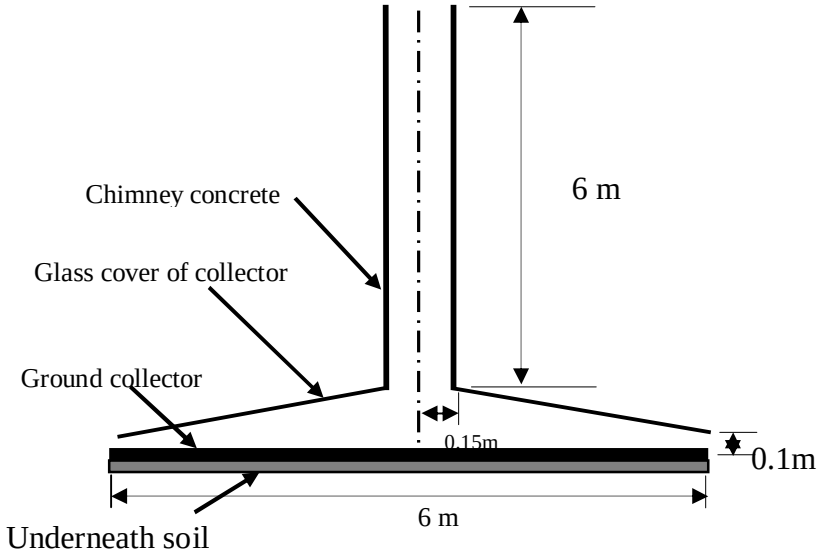

Figure 1 Schematic Diagram of the solar chimney

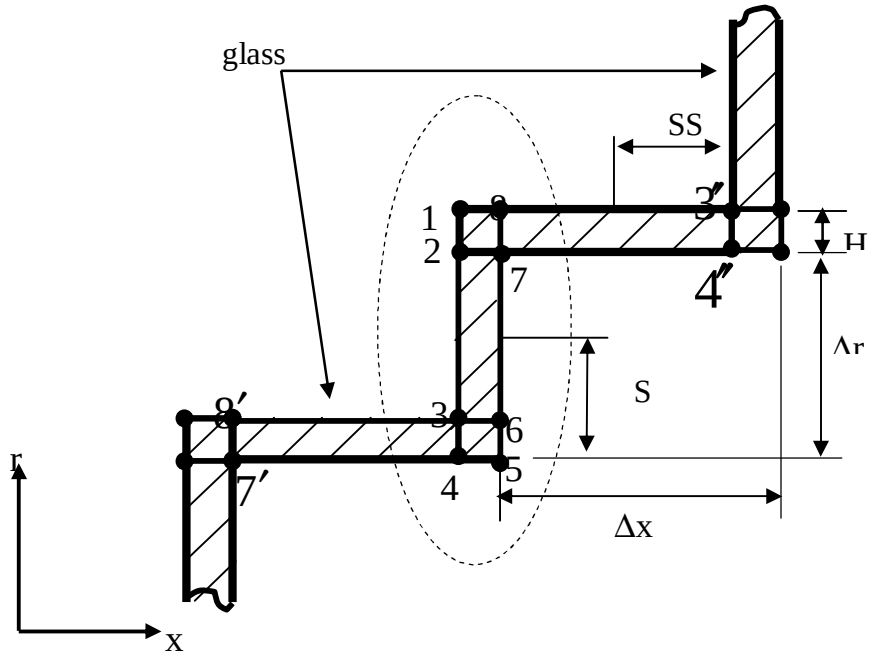

Figure (2) Section of glass as represented by simulation instead of inclined

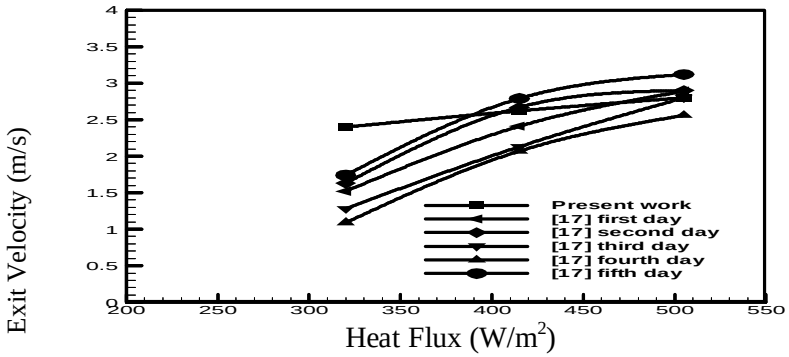

Figure (3) Comparison between numerical and experimental (Shyia, 2002) Variation of exit air velocity with heat flux for five days at L=0.1m

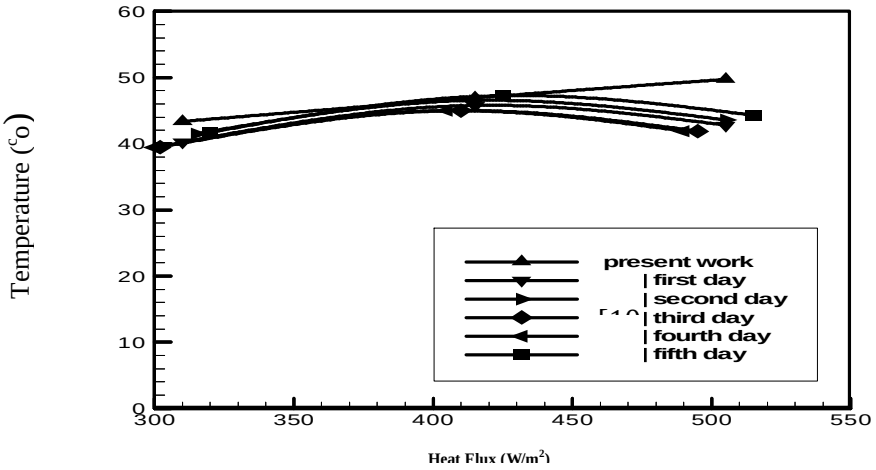

Figure (4) Comparison between numerical and experimental [10] variation of absorbing ground temperature with heat flux for five days at L = 0.1m.

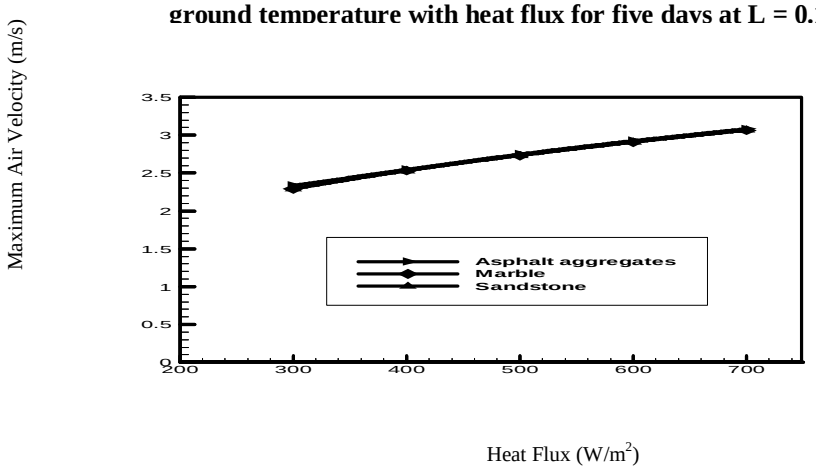

Figure (5) Variation of air velocity with heat flux for three kinds of Absorbing grounds, D = 6 m and L= 0.1m.

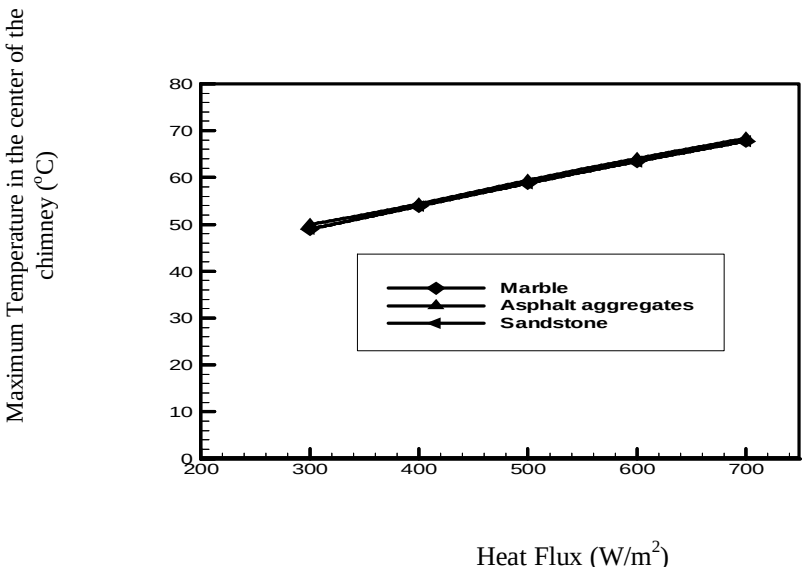

Figure (6) Variation of air temperature with heat flux for three kinds of absorbing grounds, D = 6 m and L= 0.1m.

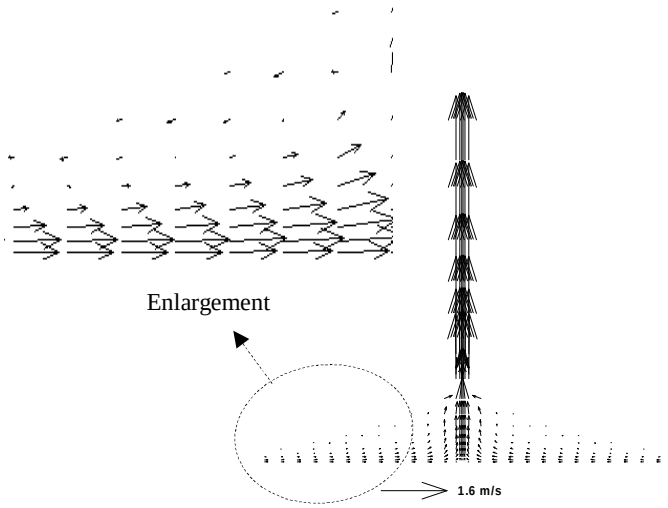

Figure (7) Flow felid of air inside solar chimney with heat flux (500 W/m^2) for black absorbing floor

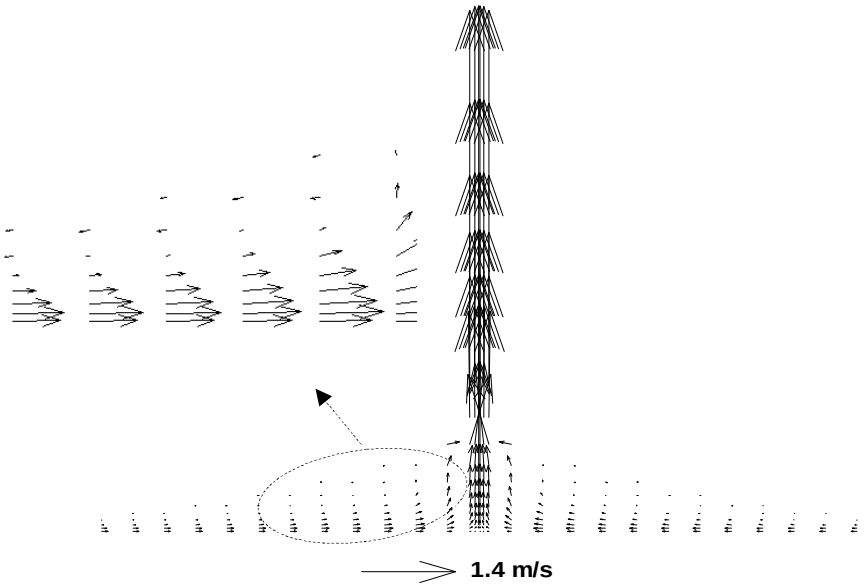

Figure (8) Flow felid of air in solar chimney with heat flux (700 W/m^2) for black absorbing floor (Asphalt aggregates), D = 9 m, L = 0.16 m.

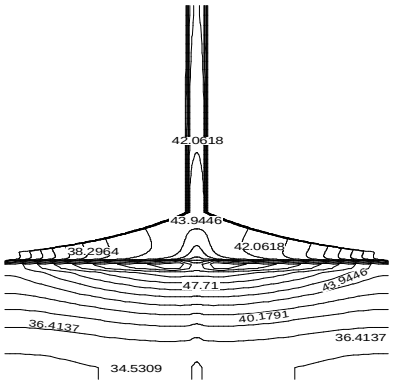

Figure (9) Isothermal contours of the complete solar chimney (air and walls) with heat flux (500 W/m^2) for black absorbing floor (Asphalt aggregates), D = 7 m, L = 0.16 m.

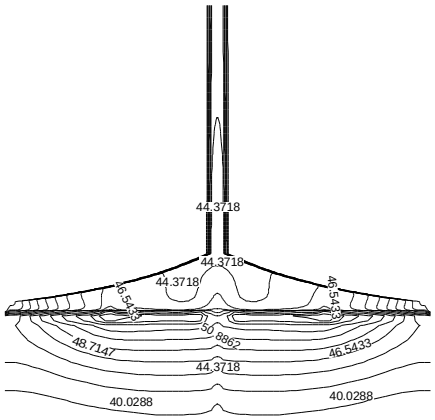

Figure (10) Isothermal contours of the complete solar chimney (air and walls) with heat flux (500 W/m^2) for black absorbing floor (Asphalt aggregates), D = 9 m, L = 0.16 m.

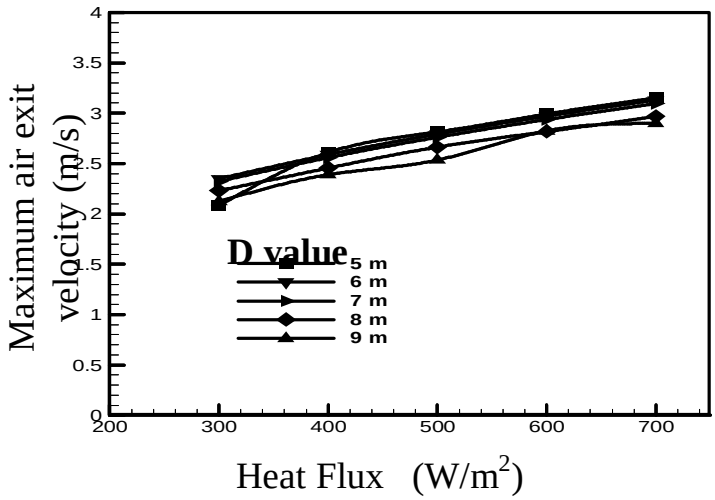

Figure (11) Variation of maximum exit air velocity at L = 0.10 m periphery height of the collector.